



Cite this: RSC Adv., 2019, 9, 36884

 Received 7th August 2019  
 Accepted 18th October 2019

DOI: 10.1039/c9ra06139h

[rsc.li/rsc-advances](http://rsc.li/rsc-advances)

## An enzyme-free FRET nanoprobe for ultrasensitive ketamine detection based on ATP-fueled target recycling†

 Hong Chen,‡ Yun Zou,‡ Xue Jiang, Fangqi Cao and Wenbin Liu \*

Ketamine is a commonly abused drug due to its stimulant, dissociative and hallucinogenic effects. An overdose of ketamine has been found to cause a variety of side effects. Therefore, the identification and quantification of ketamine are of significant importance for clinical purposes and drug seizing. However, conventional methods for ketamine detection possess some disadvantages such as sophisticated procedures, expensive instruments and low sensitivity. Herein, we develop a novel fluorescent nanoprobe for ultrasensitive ketamine detection with signal amplification based on Adenosine Triphosphate (ATP)-fueled target recycling and FRET (fluorescence resonance energy transfer) occurring between the FAM (Fluorescein, tagged with Y-shape DNA) and AuNPs. Based on the combination of FRET and signals circle amplification, the gold nanospheres functionalized with Y-motif DNA (Y@AuNPs) nanoprobe was utilized for effective ketamine detection with the limit of detection (LOD) down to 3 pg mL<sup>-1</sup>, which was lower than previously reported. Furthermore, the high sensitivity of Y@AuNPs facilitated quantitative analysis in biological media and practical samples.

### Introduction

Ketamine, (±)-2-(2-chlorophenyl)-2-(methylamino) cyclohexanone, which is a phenylcyclidine analogue mainly used as an anesthetic drug that stimulates *N*-methyl-D-aspartate (NMDA) receptors on neuronal cells.<sup>1–3</sup> It induces loss of consciousness, amnesia, immobility, pain relief and sedation while the cardiopulmonary functions and the protective airway reflexes remain unchanged.<sup>1,4,5</sup> Furthermore, ketamine is a commonly abused drug among teenagers at nightclubs and recreational parties due to its stimulant, dissociative and hallucinogenic effects.<sup>3,6,7</sup> An overdose of ketamine has been found to cause a variety of side effects such as dysfunctions of the nervous, urinary and cardiovascular systems.<sup>8,9</sup> Therefore, the identification and quantification of ketamine in biological fluids and pharmaceutical samples are of significant importance for clinical purposes and drug seizing.

To date, various techniques such as high performance liquid chromatography (HPLC),<sup>10,11</sup> gas chromatography-mass spectrometry (GC-MS),<sup>12,13</sup> liquid chromatography-mass spectrometry (LC-MS)<sup>14–16</sup> and enzyme-linked immunosorbent assay

(ELISA)<sup>17,18</sup> have been proposed for the determination of ketamine. Although most of these methods possess some advantages in practical application, they require sophisticated procedures and expensive instruments. Recently, a novel chip paper based electrochemical sensor was designed for the detection of ketamine.<sup>19,20</sup> However, the limit of detection was not satisfactory for the demand of biosample analysis.<sup>21–23</sup>

As a low-cost and accurate analytical technique, fluorescence detection based on fluorescence resonance energy transfer (FRET)<sup>24–26</sup> is promising for biosensor analysis. In addition, it can facilitate the enhancements of signals, which contributes to higher sensitivity. However, seldom work engineering FRET and enzyme-free amplification<sup>27–29</sup> is designed and employed for ketamine detection.

Herein, we developed a novel fluorescent nanoprobe with signal amplification for ketamine detection. The stimulus-responsive Y-shaped DNA termed as Y-motif<sup>30</sup> was first designed for amplifying the signal, in which ATP was utilized as endogenous fuel for signal amplification through strand displacement (Scheme 1). Then, the FAM (Fluorescein, C<sub>20</sub>H<sub>12</sub>O<sub>5</sub>)-tagged Y-motif was immobilized onto the surface of the synthesized gold nanospheres (AuNPs) by Au-S to construct the Y@AuNPs nanopropes. Meanwhile the fluorescence resonance energy transfer (FRET) occurred from the excited FAM to AuNPs, which resulted in the fluorescence quenching of FAM. With the addition of ketamine and duplex strands-DNA (dsDNA), Ya dissociated from Y-motif to hybridize with ssDNA, and the aptamer of ketamine (K-Apt) released from dsDNA to combine with ketamine, resulting that the

Shanghai Key Laboratory of Crime Scene Evidence, Shanghai Research Institute of Criminal Science and Technology, 803 Zhongshan North 1st Road, Shanghai, 200083, P. R. China. E-mail: [wbliu1981@163.com](mailto:wbliu1981@163.com); Fax: +86-21-22028361; Tel: +86-21-22028361

† Electronic supplementary information (ESI) available. See DOI: [10.1039/c9ra06139h](https://doi.org/10.1039/c9ra06139h)

‡ These authors contributed equally.



fluorescence of FAM recovered. Then, in the presence of sufficient ATP, Ya changed from chain-based structure to harpin-based structure owing to the interaction between the tail of Ya and ATP. At this time, after the combination of FRET and signals circle amplification, the Y@AuNPs nanoprobe was utilized for effective ketamine detection with the limit of detection (LOD) down to  $3 \text{ pg mL}^{-1}$ , which was lower than previously reported. Furthermore, the high sensitivity of Y@AuNPs facilitated the quantitative analysis in the biological medium and practical samples.

## Experimental

### Apparatus

UV-Vis absorption spectra were recorded on a UV spectrophotometer (Cary 60, Agilent). Fluorescence spectrum was recorded on a fluorescence spectrophotometer (F-7000, Hitachi). Morphology of AuNPs was characterized using a high-resolution transmission electron microscope (HRTEM) (JEM-2100 Hitachi, Japan).

### Chemicals and materials

Ketamine, methadone, cocaine and methamphetamine were obtained from Shanghai Research Institute of Criminal Science and Technology. Other chemicals used in this study, namely, ascorbic acid (Merck), bovine serum albumin (BSA) (Sigma-Aldrich), and sodium hydroxide (NaOH) (Merck) trisodium citrate and phosphate-buffered saline (PBS) (Sigma-Aldrich, Israel), chloroauric acid ( $\text{HAuCl}_4 \cdot 4\text{H}_2\text{O}$ ) were provided by Shanghai Chemical Reagent Company (Shanghai, China). Human blood serums ( $\geq 99\%$ ) were purchased from Solarbio Science & Technology Co., Ltd. (Beijing, China). All of DNA were synthesized by Sangon Biotech Co. Ltd. (Shanghai, China) with standard desalting and used without further purification. Tris-

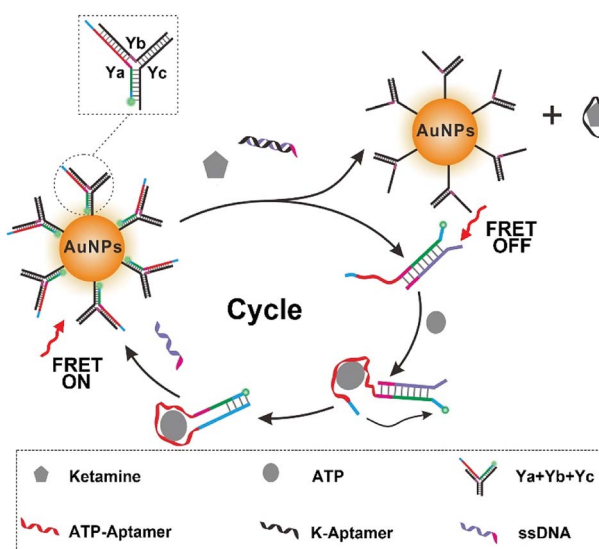
HCl (20 mM, pH = 7.6) containing 146.0 mM NaCl, 5.0 mM KCl, 5.0 mM  $\text{MgCl}_2$  was used in the DNA hybridization. The ultra-pure water with a resistivity of  $18.2 \text{ M}\Omega \text{ cm}^{-1}$  used in this work was prepared using a Milli-Q system (Hitachi, Japan). All the oligonucleotide sequences were listed in Table S1 of the ESI.† The aptamer of ketamine (K-Apt, ESI, Table S1†) was selected in our previous work using FluMag-SELEX and it could bind ketamine with high and specific abilities.<sup>31</sup>

### Preparation of 13 nm gold nanospheres (AuNPs)

We used citrate stabilized gold nanoparticle synthesis method. Specifically speaking: 7 mL of 1% trisodium citrate ( $\text{C}_6\text{H}_7\text{Na}_3\text{O}_8$ , M.W. 276.08) was added into a boiling solution of  $\text{HAuCl}_4$  (200 mL, 0.01%) under stirring. When the color of solution changes from light yellow to deep red, stop heating and continue stirring for 20 minutes. The size of AuNPs was verified by UV-Vis spectrum and TEM imaging. The synthesis AuNPs were stored at 4 °C for further use.

### Preparation of Y-motif modified AuNPs

In order to build ketamine driven signal cycle amplification system, the prepared 13 nm AuNPs were firstly functionalized with Y-motif. Typically, stoichiometric amounts of strands Ya, Yb, and Yc were mixed in Tris-HCl buffer (20 mM, pH = 7.6); the mixture was incubated at 95 °C for 5 min, and then sequentially cooled down to 65 °C, 60 °C, 55 °C, 50 °C, and 45 °C (each step for 5 min), 10  $\mu\text{L}$  of the mixture (Y-motif) were added into 100  $\mu\text{L}$  of 10 nM AuNPs. Thereafter, 12.2  $\mu\text{L}$  of citrate-HCl (20 mM, pH = 3) buffer was rapidly added into the mixture. After incubation for 30 min, the solution was centrifuged (10 000 rpm, 15 min) for three times to remove the unmodified Y-motif; the precipitate was washed for three times with Tris-



**Scheme 1** Scheme illustration of fluorescence detection mechanism and signal cycle amplification process.

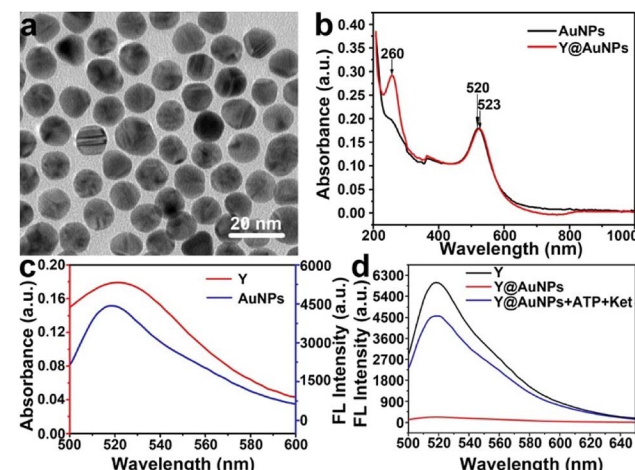


**Fig. 1** (a) Transmission electron microscopy (TEM) image. (b) Ultra-violet-Vis (UV-Vis) absorption spectra of AuNPs and Y-motif immobilized AuNPs (Y@AuNPs). (c) Principle of fluorescence resonance energy transfer (FRET). The red and blue lines are attributed to UV-Vis absorption spectra of AuNPs and fluorescence emission spectra of Y-motif. (d) Feasibility of fluorescence detection with Y@AuNPs probe. Fluorescence spectra of Y-motif (black line), Y@AuNPs (red line) and Y@AuNPs with the addition of ATP and ketamine (blue line).



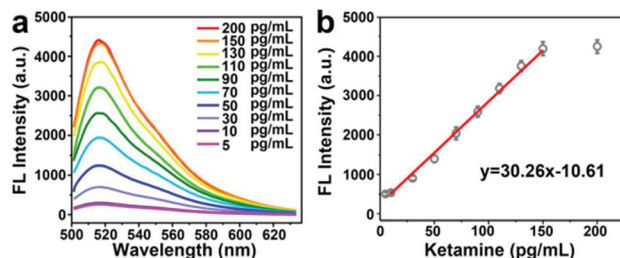


Fig. 2 (a) The fluorescence spectra of different concentrations of ketamine with Y@AuNPs in the presence of 10 mM ATP. (b) The calibration curve corresponding to (a), in which the linear equation was  $y = 30.26x - 10.61$ .

HCl (20 mM, pH = 7.6) and finally dispersed in 200  $\mu$ L Tris-HCl (20 mM, pH = 7.6). The concentration of the AuNPs was determined by measuring their absorbance at 520 nm.

### Quantitative analysis of ketamine

In order to test the sensitivity of our method, 3  $\mu$ L of 100  $\mu$ M ssDNA was firstly mixed with 3  $\mu$ L of 100  $\mu$ M ketamine aptamer and added 24  $\mu$ L Tris-HCl (20 nM, pH = 7.6). The mixed solution was incubated at 95 °C for 10 min and then cooled to room temperature. The above mixture was added into 100  $\mu$ L of 30 nM Y@AuNPs, followed by adding 50  $\mu$ L of ketamine at different concentrations (200, 150, 130, 110, 90, 70, 50, 30, 10, 5  $\text{pg mL}^{-1}$ ). To achieve the signal amplification, ATP (10 mM) was added and incubated at 37 °C for 1.5 h in Tris-HCl (20 mM, pH = 7.6). Finally, the mixture was measured under fluorescence spectrophotometer at  $\lambda_{\text{ex}}/\lambda_{\text{em}} = 492/520$  nm.

### Selectivity of the proposed probe for ketamine detection

To investigate the selectivity of the proposed nanoprobe for ketamine detection, the effect of a variety of non-specificity drugs, including 200  $\text{pg mL}^{-1}$  of methamphetamine (METH), cocaine and methadone were checked under the optimum conditions. The ketamine with the concentration of 100  $\text{pg mL}^{-1}$  was selected as the control group. The changes of relative fluorescence intensities of reaction solution were detected by fluorescence spectroscopy.

### Analysis of ketamine in blood samples

In order to investigate the possibility of the newly proposed nanoprobe to be applied for practical samples analysis, blood

serum was taken as an example in this work. First of all, 2.0 mL of methanol was added to 2.0 mL of blood sample to separate the proteins. After shaking, the mixture was centrifuged for 10 min at 3500 rpm, and then the supernatant was diluted with 2.0 mL of PBS (10 mM, pH = 7.4) and spiked with standard ketamine solution.

## Results and discussion

### Preparation and characteristics of Y@AuNPs nanoprobe

As a starting point of this work, AuNP were prepared by a hydrothermal procedure. As shown in Fig. 1a and S1 in the ESI,† the transmission electron microscopic (TEM) image shows that AuNPs are highly uniform and the average particle size is estimated to be  $13 \pm 2$  nm based on the statistics of 100 nanoparticles. The ultraviolet-Vis (UV-Vis) absorption spectrum (black line) in Fig. 1b illustrates that AuNPs display intense absorption with a peak centered at 520 nm. The UV-Vis absorption band of 520 nm of AuNPs red-shifted to 523 nm, together with a new band at 260 nm generated, indicating the Y-motif is successfully immobilized onto the surface of AuNPs to form Y@AuNPs nanoprobe.

### Principle of FRET detection for ketamine

Furthermore, the principle of FRET detection for ketamine was investigated. As shown in Fig. 1c, due to small distance between signal molecule (FAM) and AuNP and a spectral overlap between the emission spectrum of FAM centered at 520 nm and absorption spectrum of AuNP, the FRET occurred from FAM to AuNP (Fig. S2†). As shown in Fig. 1d, peaks around 525 nm were attributed to FAM. Fluorescence spectra shown in black and red lines illustrated that the fluorescence of Y-motif was quenched after the addition of AuNPs. However, in the simultaneous presence of ketamine and ATP, Ya dissociated from Y-motif to hybridize with ssDNA, and the aptamer of ketamine (K-Apt) released from dsDNA to combine with ketamine, resulting that the fluorescence of FAM recovered (blue line). Then, ATP as endogenous fuel triggered the next round. In this manner, the signal can be amplified, which was beneficial for detecting trace ketamine. These results indicated the feasibility of Y@AuNPs nanoprobe for fluorescence detection of ketamine.

### Optimization of detection conditions

To evaluate the detection ability of Y@AuNPs nanoprobe for ketamine, the concentration of ATP was first studied. Fig. S3†

Table 1 Comparison of performance of different methods for detection of ketamine

Detection methods	Sample	Detection limit	Reference
Electro-microchip	Urine-plasma	50 $\text{ng mL}^{-1}$	25
LC/MS/MS	Hair	20 $\text{ng g}^{-1}$	26
UPLC	Urine	0.1 $\text{ng mL}^{-1}$	18
GC-MS	Urine	0.5-1.0 $\text{ng mL}^{-1}$	9
Fluorescence	Blood	60 $\text{pg mL}^{-1}$	32
FRET and signal amplification	Blood	3 $\text{pg mL}^{-1}$	This article



revealed that the strand displacement kinetics was finely controlled by varying the concentrations of ATP. The signals were efficiently enhanced with the fueling ATP in the range from 1 mM to 10 mM. In addition, upon the addition of ketamine (200  $\mu\text{g mL}^{-1}$ ) and excess ATP, fluorescence intensity of FAM gradually increased with the prolong time, and remained unchanged until 1.5 h (Fig. S4†). Thus, the reaction time was optimized to be 1.5 h. Then, the stability of Y@AuNPs under various pH was demonstrated in Fig. S5.† The fluorescence intensity of FAM was observed to retain stable in the pH range of 3.0–11.0 in the presence of 120  $\mu\text{g mL}^{-1}$  ketamine. In consideration of human physiological environment, pH 7.6 was chosen as the optimal one in the following experimental procedures.

### Quantitative measurement of ketamine

Based on the above optimized conditions, the detection ability of Y@AuNPs for ketamine was further investigated. As shown in Fig. 2a, in the presence of 10 mM ATP, the fluorescence intensity of FAM increased gradually with the increasing concentration of ketamine. Meanwhile, the fluorescence intensity exhibited good linearity with the concentration of ketamine in the range from 10  $\mu\text{g mL}^{-1}$  to 150  $\mu\text{g mL}^{-1}$  with the limit of detection (LOD) of 3  $\mu\text{g mL}^{-1}$  at  $3\sigma$ . The LOD of the developed Y@AuNPs for ketamine was compared with those of other works reported previously, with the comparison results shown in Table 1. In previous studies, the estimated detection limit of ketamine in blood using novel fluorescence genosensor is 0.06  $\text{ng mL}^{-1}$ . Accordingly, the developed fluorescent nanoprobe can display better detection ability.

### Selectivity analysis of Y@AuNPs for ketamine detection

Then, the specificity of this Y@AuNPs nanoprobe was further evaluated by comparing the fluorescence signal response measured for these four kinds of drugs, including target ketamine (100  $\mu\text{g mL}^{-1}$ ), methadone, cocaine and methylamphetamine (METH) at the same concentration of 200  $\mu\text{g mL}^{-1}$ . As shown in Fig. 3a and b, the relative fluorescence intensities change of Y@AuNPs for the interfering substances (methadone, cocaine and METH) were very small, while ketamine showed significant increase of fluorescence. These

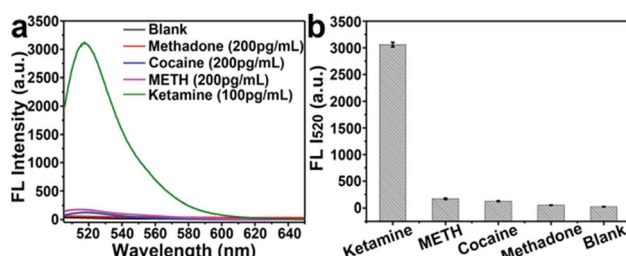


Fig. 3 (a) Evolution of the selectivity. The fluorescence spectra of the ketamine detection system toward the four various drugs including ketamine (100  $\mu\text{g mL}^{-1}$ ), methadone, cocaine and methamphetamine (METH) with the concentration of 200  $\mu\text{g mL}^{-1}$ . (b) The corresponding fluorescence bars chart for specificity detection.

Table 2 Determination of ketamine in human blood samples ( $n = 5$ )

Sample	Detected ( $\mu\text{g mL}^{-1}$ )	Added ( $\mu\text{g mL}^{-1}$ )	Recovery (%)	RSD (%)
Blood	—	Blank	—	—
	11.8	10	118	4.5
	31.8	30	106	3.7
	48.5	50	97	4.8
	93	100	93	3.3
	135	150	90	2.6

results indicated that our designed probe exhibited a good selectivity to discriminate ketamine and the other drugs.

### Quantitative analysis of ketamine in simulated blood samples

The excellent detection ability of Y@AuNPs enabled it to be a reliable approach for quantitative analysis in biological medium. For practical application, the fluorescence sensor for ketamine detection in blood samples was performed using the standard addition method. The certain amounts of ketamine were added to the prepared samples and the ketamine concentration was measured by the proposed sensor. Five measurements were performed at each concentration. The experimental results were summarized in Table 2. As depicted, the obtained recoveries were in the range of 95–110% with RSDs less than 4.2%, which demonstrated the capability of the proposed Y@AuNPs for determination of ketamine in biological samples.

## Conclusions

In summary, we have successfully developed a novel Y@AuNPs fluorescent nanoprobe composed of AuNP and Y-motif DNA structure for ketamine detection by FRET effect. The sufficient ATP in biological medium was termed as fuel, which can realize the signal amplification for improving the sensitivity for ketamine detection in coordination with Y-motif. The LOD was down to 3  $\mu\text{g mL}^{-1}$ , which was lower than previously reported. In addition, the nanoprobe showed good selectivity towards ketamine. Furthermore, the acceptable recoveries which obtained from the practical sample analysis, revealed that the performance of the developed nanoprobe was not affected significantly by the matrix of the practical samples and the proposed Y@AuNPs can be used for determination of ketamine in blood samples.

### Conflicts of interest

There are no conflicts to declare.

### Acknowledgements

This work was sponsored by Shanghai Scientific and Technological Innovation Project (16dz1205600, 17DZ1205400 and 19dz1200400), Program of Shanghai Academic/Technology



Research Leader (19XD1432700), Shanghai Rising-Star Program (18QB1403400 and 19QB1405200), National Natural Science Foundation of China (21704110), Natural Science Foundation of Shanghai (19ZR1449500 and 19ZR1449400), Science and Technology Development Fund of Shanghai Municipal Public Security Bureau (2018002 and 2018003), which we gratefully acknowledged.

## References

- 1 P. S. K. Chu, W. K. Ma, S. C. W. Wong, R. W. H. Chu, C. H. Cheng, S. Wong, J. M. I. Tse, F. L. Lau, M. K. Yiu and C. W. Man, The destruction of the lower urinary tract by ketamine abuse: A new syndrome, *BJU Int.*, 2010, **102**, 1616–1622.
- 2 J. M. Felser and D. J. Orban, Dystonic reaction after ketamine abuse, *Ann. Emerg. Med.*, 1982, **11**, 673–675.
- 3 A. C. Lahti, M. A. Weiler, B. T. Michaelidis, A. Parwani and C. A. Tamminga, Effects of ketamine in normal and schizophrenic volunteers, *Neuropsychopharmacology*, 2001, **25**, 455–467.
- 4 R. M. Berman, A. Cappiello, A. Anand, D. A. Oren, G. R. Heninger, D. S. Charney and J. H. Krystal, Antidepressant effects of ketamine in depressed patients, *Biol. Psychiatry*, 2000, **47**, 351–354.
- 5 J. H. Krystal, L. P. Karper, J. P. Seibyl, G. K. Freeman, R. Delaney, J. D. Bremner, G. R. Heninger, M. B. Bowers and D. S. Charney, Subanesthetic effects of the noncompetitive NMDA antagonist, ketamine, in humans. Psychotomimetic, perceptual, cognitive, and neuroendocrine responses, *Arch. Gen. Psychiatry*, 1994, **51**, 199–214.
- 6 Q. Deng, Q. Tang, R. S. Schottenfeld, W. Hao and M. C. Chawarski, Drug use in rural China: a preliminary investigation in Hunan Province, *Addiction*, 2012, **107**, 610–613.
- 7 K. Xu and R. H. Lipsky, Repeated ketamine administration alters N-methyl-D-aspartic acid receptor subunit gene expression: implication of genetic vulnerability for ketamine abuse and ketamine psychosis in humans, *Exp. Biol. Med.*, 2015, **240**, 145–155.
- 8 H. V. Curran and L. Monaghan, In and out of the K-hole: a comparison of the acute and residual effects of ketamine in frequent and infrequent ketamine users, *Addiction*, 2001, **96**, 749–760.
- 9 J. M. White and C. F. Ryan, Pharmacological properties of ketamine, *Drug Alcohol Rev.*, 1996, **15**, 145–155.
- 10 Y. Fan, Y. Q. Feng, S. L. Da and X. P. Gao, In-tube solid-phase microextraction with poly(methacrylic acid-ethylene glycol dimethacrylate) monolithic capillary for direct high-performance liquid chromatographic determination of ketamine in urine samples, *Analyst*, 2004, **129**, 1065–1069.
- 11 P. Li, H. Han, X. Zhai, W. He, L. Sun and J. Hou, Simultaneous HPLC-UV determination of ketamine, xylazine, and midazolam in canine plasma, *J. Chromatogr. Sci.*, 2012, **50**, 108–113.
- 12 M. K. Huang, C. Liu, J. H. Li and S. D. Huang, Quantitative detection of ketamine, norketamine, and dehydronorketamine in urine using chemical derivatization followed by gas chromatography-mass spectrometry, *J. Chromatogr. B: Anal. Technol. Biomed. Life Sci.*, 2005, **820**, 165–173.
- 13 H. R. Lin and A. C. Lua, A fast GC-MS screening procedure for ketamine and its metabolites in urine samples, *J. Food Drug Anal.*, 2005, **13**, 107–111.
- 14 L. G. Apollonio, D. J. Pianca, I. R. Whittall, W. A. Maher and J. M. Kyd, A demonstration of the use of ultra-performance liquid chromatography-mass spectrometry [UPLC/MS] in the determination of amphetamine-type substances and ketamine for forensic and toxicological analysis, *J. Chromatogr. B: Anal. Technol. Biomed. Life Sci.*, 2006, **836**, 111–115.
- 15 J. Y. Cheng and V. K. Mok, Rapid determination of ketamine in urine by liquid chromatography-tandem mass spectrometry for a high throughput laboratory, *Forensic Sci. Int.*, 2004, **142**, 9–15.
- 16 I. R. Miksa, M. R. Cummings and R. H. Poppenga, Determination of acepromazine, ketamine, medetomidine, and xylazine in serum: multi-residue screening by liquid chromatography-mass spectrometry, *J. Anal. Toxicol.*, 2005, **29**, 544–551.
- 17 P. S. Cheng, C. Y. Fu, C. H. Lee, C. Liu and C. S. Chien, GC-MS quantification of ketamine, norketamine, and dehydronorketamine in urine specimens and comparative study using ELISA as the preliminary test methodology, *J. Chromatogr. B: Anal. Technol. Biomed. Life Sci.*, 2007, **852**, 443–449.
- 18 J. H. Watterson and T. C. J. VandenBoer, Effects of tissue type and the dose-death interval on the detection of acute ketamine exposure in bone and marrow with solid-phase extraction and ELISA with liquid chromatography-tandem mass spectrometry confirmation, *J. Anal. Toxicol.*, 2008, **32**, 63–638.
- 19 V. B. C. Lee, N. F. Mohd-Naim, E. Tamiya and M. U. Ahmed, Trends in paper-based electrochemical biosensors: from design to application, *Anal. Sci.*, 2018, **34**, 7–18.
- 20 J. Narang, N. Malhotra, C. Singhal, A. Mathur, D. Chakraborty, A. Anil, A. Ingle and C. S. Pundir, Point of care with micro fluidic paper based device integrated with nano zeolite-graphene oxide nanoflakes for electrochemical sensing of ketamine, *Biosens. Bioelectron.*, 2017, **88**, 249–257.
- 21 T. Kawasaki, M. Ogata, C. Kawasaki, J. I. Ogata, Y. Inoue and A. Shigematsu, Ketamine suppresses proinflammatory cytokine production in human whole blood in vitro, *Anesth. Analg.*, 1999, **89**, 665.
- 22 A. C. Lahti, H. H. Holcomb, D. R. Medoff and C. A. Tamminga, Ketamine activates psychosis and alters limbic blood flow in schizophrenia, *NeuroReport*, 1995, **6**, 869–872.
- 23 K. A. Moore, J. Sklerov, B. Levine and A. J. Jacobs, Urine concentrations of ketamine and norketamine following illegal consumption, *J. Anal. Toxicol.*, 2001, **25**, 583–588.



24 R. Heim and R. Y. Tsien, Engineering green fluorescent protein for improved brightness, longer wavelengths and fluorescence resonance energy transfer, *Curr. Biol.*, 1996, **6**, 178–182.

25 X. L. Zhang, Y. Xiao and X. H. Qian, A Ratiometric Fluorescent Probe Based on FRET for Imaging  $Hg^{2+}$  Ions in Living Cells, *Angew. Chem., Int. Ed.*, 2008, **47**, 8025–8029.

26 H. Tian, L. Ip, H. Luo, D. Chang and K. Luo, A high throughput drug screen based on fluorescence resonance energy transfer (FRET) for anticancer activity of compounds from herbal medicine, *Br. J. Pharmacol.*, 2007, **150**, 321–334.

27 L. Li, J. Feng, H. Liu, Q. Li, L. Tong and B. Tang, Two-color imaging of microRNA with enzyme-free signal amplification via hybridization chain reactions in living cells, *Chem. Sci.*, 2015, **7**, 1940–1945.

28 L. Yang, C. Liu, W. Ren and Z. Li, Graphene surface-anchored fluorescence sensor for sensitive detection of microRNA coupled with enzyme-free signal amplification of hybridization chain reaction, *ACS Appl. Mater. Interfaces*, 2012, **4**, 6450–6453.

29 A. X. Zheng, J. Li, J. R. Wang, X. R. Song, G. N. Chen and H. H. Yang, Enzyme-free signal amplification in the DNAzyme sensor via target-catalyzed hairpin assembly, *Chem. Commun.*, 2012, **48**, 3112–3114.

30 P. Zhang, C. Wang, J. Zhao, A. Xiao, Q. Shen, L. Li, J. Li, J. Zhang, Q. Min and J. Chen, Near infrared-guided smart nanocarriers for microRNA-controlled release of doxorubicin/siRNA with intracellular ATP as fuel, *ACS Nano*, 2016, **10**, 3637–3647.

31 M. Sun, F. Cao, X. Hu, Y. Zhang, X. Lu and L. Zeng, DNA Aptamer Selection *in vitro* for Determining Ketamine by FluMag-SELEX, *J. Forensic Med.*, 2014, **30**, 346–349.

32 Y. Ding, X. Li, Y. Guo, J. Yan, J. Ling, W. Li and L. Zha, Rapid and sensitive detection of ketamine in blood using novel fluorescence genosensor, *Anal. Bioanal. Chem.*, 2017, **409**, 7027–7034.

